Earth and Planetary Science Letters 315–316 (2012) 41–50

Contents lists available at ScienceDirect

Earth and Planetary Science Letters

journal homepage: www.elsevier.com/locate/epsl

Synchronizing a sea-level jump, final Lake Agassiz drainage, and abrupt cooling 8200 years ago

Yong-Xiang Li [a,*], Torbjörn E. Törnqvist [a,b], Johanna M. Nevitt [a,1], Barry Kohl [a]

[a] Department of Earth and Environmental Sciences, Tulane University, New Orleans, LA 70118-5698, USA
[b] Tulane/Xavier Center for Bioenvironmental Research, Tulane University, New Orleans, LA 70118-5698, USA

ARTICLE INFO

Article history:
Accepted 18 May 2011
Available online 12 June 2011

Editor: P. DeMenocal

Keywords:
8.2 ka event
sea level
abrupt climate change
Mississippi Delta

ABSTRACT

Freshwater pulses draining into the North Atlantic Ocean are commonly hypothesized to have perturbed the Atlantic meridional overturning circulation (MOC), triggering abrupt climate changes such as Heinrich events, the Younger Dryas, and the 8.2 ka event. However, dating uncertainties have prevented causal links between freshwater pulses and climate events from being firmly established. Here we report a high-resolution relative sea-level record from the Mississippi Delta that documents a sea-level jump that occurred within the 8.18 to 8.31 ka (2σ) time window and is attributed to the final drainage of proglacial Lake Agassiz–Ojibway (LAO). This age is indistinguishable from the onset of the 8.2 ka climate event, consistent with a nearly immediate ocean–atmosphere response to the freshwater perturbation. This constitutes a rare currently available example of a major abrupt climate cooling that can be directly linked to a well-documented freshwater source with a temporal resolution on the order of a century. The total inferred eustatic sea-level rise associated with the very final stage of LAO drainage at 8.2 ka ranges from 0.8 to 2.2 m, considerably higher than previous estimates. These new constraints on the timing and amount of final LAO drainage permit significantly improved quantitative analysis of the sensitivity of MOC to freshwater perturbation, a crucial step toward understanding abrupt climate change.

1. Introduction

Abrupt climate change has received extensive interest for a wide range of reasons, including its potential role in a future warming world (Alley et al., 2003). Over the past few decades, the connection between freshwater forcing and abrupt climate change due to perturbation of the Atlantic meridional overturning circulation (MOC) has enjoyed widespread popularity, since it offers a potential mechanism to explain phenomena such as Heinrich events (Heinrich, 1988), the Younger Dryas (Broecker et al., 1989), and the 8.2 ka event (Barber et al., 1999). However, the past few years have seen this hypothesis becoming increasingly challenged (e.g., Broecker et al., 2010; Fisher et al., 2008; Lowell et al., 2009), in part reflecting the fact that very few abrupt climate events have been unequivocally linked to a well-mapped and well-dated freshwater source (cf. Clement and Peterson, 2008).

The 8.2 ka cold event is the most prominent abrupt North Atlantic climate change of the Holocene and is increasingly recognized in many other parts of the world (Alley and Águstsdóttir, 2005; Cheng et al., 2009). This event is often believed to have resulted from the final outburst of proglacial Lake Agassiz–Ojibway (LAO) when an ice dam over Hudson Bay collapsed (Barber et al., 1999; Lajeunesse and St-Onge, 2008) and the rapid drainage flooded the North Atlantic Ocean with freshwater and perturbed the Atlantic MOC (Ellison et al., 2006; Kleiven et al., 2008), leading to widespread cooling. In addition, the rerouting of western Canadian Plains runoff following the collapse of the ice dam over Hudson Bay may have contributed to the 8.2 ka climate event (Carlson et al., 2009). Despite the popularity of a causal link between the final LAO drainage and the 8.2 ka climate event, this relationship has yet to be firmly demonstrated because the catastrophic LAO drainage remains poorly constrained in terms of its timing and amount. The only available direct dating of the final LAO drainage yields an age range of 8.16 to 8.74 ka at the 1σ level (Barber et al., 1999). This large age uncertainty precludes an unequivocal connection between LAO drainage and the 8.2 ka event and allows for alternative hypotheses such as a role for solar forcing around this time interval (Muscheler et al., 2004; Rohling and Pälike, 2005). Also, the amount of LAO drainage is not well known as reflected by highly variable estimates (e.g., Barber et al., 1999; Hijma and Cohen, 2010; Leverington et al., 2002; Törnqvist et al., 2004a), inhibiting our understanding of the sensitivity of MOC to freshwater perturbation.

This study seeks to refine previous work (Törnqvist et al., 2004a) that provided the first evidence for a sea-level jump around 8.2 ka based on stratigraphic data from the Mississippi Delta, Louisiana, USA.

* Corresponding author at: School of Earth Sciences and Engineering, Nanjing University, Nanjing 210093, China.
E-mail address: yxli@nju.edu.cn (Y.-X. Li).
[1] Present address: School of Earth Sciences, Stanford University, Stanford, CA 94305, USA.

0012-821X/$ – see front matter © 2011 Elsevier B.V. All rights reserved.
doi:10.1016/j.epsl.2011.05.034

We present a high-resolution relative sea-level (RSL) record around this time interval using basal peat to track sea-level change. The rationale of this approach is that rising seas drown the coastal landscape and transform it into a peat-forming wetland that accumulates over a consolidated, compaction-free Pleistocene basement. Therefore, intertidal basal peats can be used to determine past sea levels with high accuracy via precise measurements of their age and elevation. The robustness of this approach has been demonstrated in a variety of coastal settings (e.g., Donnelly et al., 2004; Jelgersma, 1961).

2. Study area

Coastal plains worldwide (e.g., the US Atlantic Coast) rarely capture the age/depth range necessary to sample early Holocene sea-level records that are more likely found in large, prograding deltas. However, not all deltas contain basal peat and even fewer also occur in microtidal settings which are particularly favorable for high-resolution sea-level studies. Our sampling sites are located in the Bayou Sale area in the western part of the Mississippi Delta (Fig. 1). The US Gulf Coast is characterized by a microtidal regime with a present-day spring tidal range typically <0.5 m in coastal Louisiana. In addition, the study area has been tectonically relatively stable during the Holocene (Törnqvist et al., 2006). Glacial isostatic adjustment (GIA) contributes significantly to RSL rise in this area around 8.2 ka (Kendall et al., 2008), but the GIA component would be negligible during a short-lived sea-level jump. This overall combination of circumstances makes our study area exceptionally well suited to resolve dm-scale RSL changes for this time interval.

The Pleistocene basement in the study area consists of the pervasively oxidized Prairie Complex (Autin et al., 1991) that is capped by a few meters of Peoria Loess. Both units are highly consolidated and essentially compaction-free due to prolonged subaerial exposure. Overlying the Peoria Loess is an immature paleosol consisting of an A-horizon enriched in highly decomposed organic matter. This paleosol was classified as an Entisol, suborder Aquent, by Törnqvist et al. (2004b) and is the result of transgression, a rising groundwater table, and the initial transformation of the landscape into a wetland environment. The continued rise of the groundwater table eventually enabled the formation of basal peat. The distinction between the paleosol and the basal peat is based on (1) the dark gray matrix color for the paleosol vs. gray brown for the basal peat; (2) the lesser degree of organic matter decomposition in the peat as reflected by abundant herbaceous plant fibers; and (3) the massive structure of the paleosol compared to the faintly laminated peat. Nevertheless, basal peat can have a significant mud content and occasionally contains distinct mud beds.

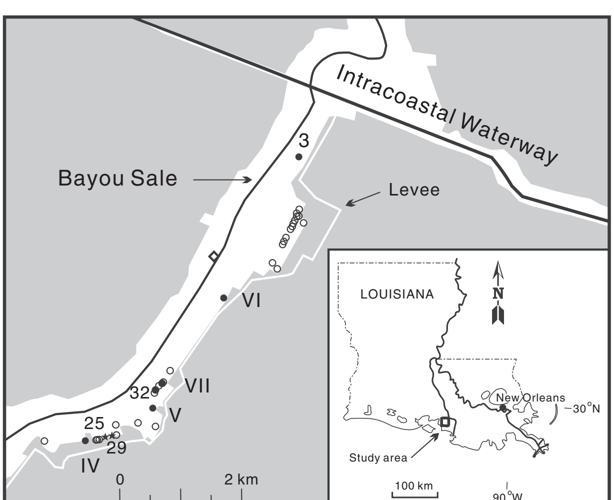

Fig. 1. Map of the Bayou Sale study area and core sites. Filled circles indicate the sites shown in Fig. 2 that contain basal peat. Asterisks represent sites with a sharp transition from paleosol to lagoonal mud with no basal peat. Open circles denote the other core sites listed in Table 1. The open diamond indicates the location of the NGS benchmark (T168, elevation of + 1.83 m with respect to North American Vertical Datum 88).

3. Methods

We collected cores with a Geoprobe system (model 6610 DT). The early stage of coring aimed at mapping the stratigraphy along a ~6-km-long transect (Fig. 1), exhibiting a transgressive surface associated with the Pleistocene–Holocene transition. Subsequent efforts were focused on coring at key locations for detailed sampling to improve the precision of depth measurements of this transgressive surface.

Cores were initially described in the field and then transported to Tulane University for cold storage (~4 °C). In the laboratory, representative cores containing basal peat were sampled for radiocarbon dating, carbon isotope measurements, and foraminiferal analysis to determine the chronology of basal peat and to constrain depositional environments of both basal peat and adjacent strata. Radiocarbon dating of terrestrial plant remains from basal peat was performed by accelerator mass spectrometry (AMS) at the University of California, Irvine. Stable carbon isotope and foraminiferal analyses of two representative cores (sites Bayou Sale VI and IV) were performed to characterize depositional environments. For $\delta^{13}C$ analysis, samples were first dried at 60 °C for 24 h and acidified with 10% HCl to remove carbonates. The residues were centrifuged and the isolated organic material was then dried overnight at 60 °C. $\delta^{13}C$ measurements were carried out at the Stable Isotope Laboratory at the University of Miami. For the foraminiferal analysis, samples were soaked in water for 24 h, wet sieved, and the >63 μm fraction was examined under a microscope. Identification of agglutinated foraminifera was based mainly on pseudo-chitinous linings because complete outer tests were often lacking due to poor preservation.

Optical surveys with an infrared TOPCON GTS-4B total station were conducted between core sites and National Geodetic Survey (NGS) benchmark T168 (UTM-coordinates: N = 3281.840; E = 645.980) (Fig. 1) to determine the land surface elevation at the core sites. In addition, temporary benchmarks were established between the NGS benchmark and core sites. The temporary benchmarks (not shown in Fig. 1) were located very close (typically <100 m) to the core sites. At least two round-trip surveys were carried out between the NGS benchmark and temporary benchmarks, and typically two round-trip surveys were conducted between a temporary benchmark and a core site. The cumulative error for a round-trip elevation survey between the NGS benchmark and core sites is within 0.05 m.

4. Results

4.1. Stratigraphy

We drilled 37 sites along the ~6-km-long transect to map the stratigraphy in the Bayou Sale area (Fig. 1); key stratigraphic information for all core sites is summarized in Table 1. Multiple cores that capture the Pleistocene–Holocene transition were drilled at the majority of the sites.

The transgressive succession at the stratigraphically deeper sites (V, 32, VII, and VI) is characterized by a basal-peat bed that caps the dark gray paleosol described above and is abruptly overlain by pale-gray, shell-bearing muds (Figs. 2, 3). The basal-peat bed at the deepest sites (V, 32 and VII) shows highly variable characteristics and thicknesses among multiple cores at each site and is often absent in this deeper portion of the record due to erosion (Table 1). This is

Table 1
Summary of the Pleistocene–Holocene transition features in the Bayou Sale area, western Mississippi Delta.

Elevation (m)[a]	Borehole number[b]	UTM coordinates		Transition facies	Number of observations
		N	E		
N/A	0792.002	3281.500	646.980		1
N/A	0892.011	3282.320	647.320		2
N/A	0892.028	3279.040	644.000		1
−12.22	0892.013	3281.960	647.080	M	3
−12.34	0892.003	3282.140	647.180	M	2
−12.51	0892.002	3282.020	647.100	M	4
−12.76	0892.014	3282.400	647.380	M	6
−13.10	0892.015	3282.380	647.440	M	2
−13.11	0892.012	3282.300	647.300	M	1
−13.12	0892.017	3282.360	647.460	M	1
−13.14	0892.010	3282.260	647.280	M	5
−13.25	0892.018	3282.500	647.420	M	2
−13.45	0792.003 (3)	3283.420	647.640	M	14
−13.57	0792.001	3282.320	647.520	M	1
−13.68	0892.023	3279.120	643.620	M	1
−14.01	0892.027	3279.020	643.860	M	1
−14.05	0892.022	3279.100	643.560	M	1
−14.07	0892.026	3279.020	643.880	M	6
−14.08	0892.004 (IV)	3279.020	643.580	M	10
−14.11	0892.030	3279.000	643.780	M	1
−14.14	0892.025 (25)	3279.000	643.960	L	6
−14.16	0892.024	3279.020	643.840	M[c]	1
−14.18	0892.031	3279.040	643.960	L	1
−14.39	0892.029 (29)	3279.040	643.980	L	6
−14.41	0892.007 (VI)	3281.100	646.080	LP	7
−14.75	0892.020	3279.260	644.460	LE	3
−15.09	0892.019	3279.160	644.080	LE	3
−15.42	0892.006	3278.960	642.820	LP	2
−15.44	0892.008	3280.040	645.060	LE	1
−15.54	0892.035 (VII)	3279.920	644.980	LP,LE	3
−15.57	0892.001	3281.700	646.880	LE	4
−15.61	0892.009	3279.800	644.820	LP	1
−15.69	0892.034	3279.940	645.000	LE	1
−15.87	0892.032 (32)	3279.800	644.840	LP, LE	5
−15.89	0892.021	3279.100	644.780	LE	3
−16.02	0892.033	3279.880	644.920	LP	1
−16.07	0892.005 (V)	3279.400	644.760	LP, LE	10

M = marsh mud/peat on paleosol, L = lagoonal mud on paleosol, LP = lagoonal mud on peat on paleosol; LE = lagoonal mud erosive into paleosol or underlying strata.

[a] Elevation is calculated with respect to NAVD 88; Elevation "N/A" indicates that the transition is not well defined at the site.

[b] Number in parentheses indicates sites shown in Fig. 2.

[c] Elevation is based only on one observation and is not as precise as those at sites 0892.025 and 0892.029 where multiple observations were obtained.

illustrated by site V where multiple cores (Fig. 3), all drilled within an area of a few square meters, include a well preserved basal-peat bed (core H) as well as clear signs of erosion and redeposition as witnessed by mud clasts (core A), a completely reworked stratigraphy (core F) or complete erosion of the basal peat (core D) and possibly even the uppermost paleosol (cores D and F). This provides compelling evidence that the initially formed basal peat was highly susceptible to erosion associated with the rapid transgression.

The transgressive succession at the stratigraphically shallowest sites (IV and 3) is characterized by a basal-peat bed that gradually gives way to overlying brown-gray muds (Figs. 2, 3), comparable to what was observed at all core sites with a Pleistocene–Holocene transition <14 m below present sea level (Table 1). Unlike the deeper sites discussed above, shells or shell fragments are completely absent in the brown-gray mud that overlies the basal peat at the stratigraphically shallower sites (IV and higher) (Figs. 2, 3). Instead, the brown-gray mud is characterized by faintly laminated organic-rich beds with plant matter reminiscent of the constituents of the underlying basal peat.

The transgressive surface at intermediate depth intervals is recorded at sites 25 and 29 and exhibits a unique signature not seen in the remainder of the record (Table 1). At these sites, shell-rich muds immediately onlap the underlying paleosol with no basal peat between the paleosol and the muds (Figs. 2, 3). While the transition is sharp, these deposits do not contain reworked organic matter, and, hence, suggest that the transition is conformable (Fig. 3).

4.2. Paleoenvironmental reconstruction

The depositional environments associated with the facies described above are reconstructed by means of foraminiferal and stable carbon isotope analysis. Fig. 4a shows the succession of foraminiferal assemblages and other microfossils at site Bayou Sale VI. The basal-peat bed and the underlying paleosol are dominated by the agglutinated taxa *Haplophragmoides wilberti* and *Ammoastuta inepta*. This interval is interpreted to represent a brackish marsh environment. In the mud above the basal peat, the microfauna is dominated by calcareous foraminifera of the taxa *Ammonia beccarii sl.* and *Elphidium gunteri*, with *Ammobaculites* spp. being the next dominant genus along with occurrences of *H. wilberti*. *Ammobaculites* spp. is represented only by the early coiled portion of the test and therefore no species identification was possible. The calcareous foraminifera (*Ammonia* and *Elphidium*) occur in open water where salinities are generally greater than 10 ppt (Kane, 1967). The interval above the peat is therefore interpreted to represent an open-water, brackish lagoonal environment. Fragments of pelecypod taxa *Rangia cuneata* and *Macoma mitchelli*, characteristic of shallow brackish environments with salinities of 2–15 ppt (Parker, 1959; Phleger, 1965; LaSalle and de la Cruz, 1985) occur just above the basal peat (Fig. 1; sites VI, V, VII, and 32), providing additional evidence that the brackish marsh was abruptly replaced by a brackish lagoon.

Fig. 4b shows the succession of foraminiferal taxa and other microfossils at site Bayou Sale IV. The section below 14.0 m is dominated exclusively by *H. wilberti* and interpreted as a brackish marsh environment. The interval above 14.0 m is represented by a *H. wilberti*–*A. inepta* assemblage and is also interpreted as a brackish marsh, possibly with a lower salinity due to the occurrence of *A. inepta*. Scott et al. (1991) recorded *A. inepta* in Louisiana marshes with salinities ranging from 3 to 5 ppt. *H. wilberti* and *A. inepta* are represented in most samples only by their pseudochinous linings. In one sample (13.76 m) whole specimens with the fragile test intact were preserved, allowing for positive identification of the species and associated linings. The general environmental setting is similar to that described by Kane (1967) where a *H. wilberti*–*A. inepta* assemblage occurs as part of a fringe marsh with salinities less than 10 ppt.

The basal peat at sites VI and IV yielded δ^{13}C values of −13.0‰ and −12.9 to −15.6‰, respectively, also indicative of a brackish marsh environment (Chmura et al., 1987). The combined micropaleontological and geochemical data provide conclusive evidence that the basal peat at both sites accumulated within the intertidal zone (between mean tide level and mean spring high water). While at site IV this environment persisted up section, at site VI the marsh was abruptly replaced by an open-water, brackish lagoon. Given the straightforward relationship between microfossil content and lithofacies, all cores presented in this study (Table 1, Fig. 1) can be readily interpreted in terms of depositional environments.

4.3. Elevation and sea-level relationship of basal peat

The elevation of past sea level was calculated using depth measurements, elevation surveys, and the vertical indicative range (*sensu* Van de Plassche, 1986) of basal peat with respect to sea level. The depth is defined as the contact between the basal-peat bed and the underlying paleosol. Since basal peats were deposited on the highly consolidated Pleistocene substrate, this essentially eliminates elevation errors induced by post-depositional compaction. Multiple cores were collected from each site to determine the measurement error of the depth level of basal-peat beds (Table 2).

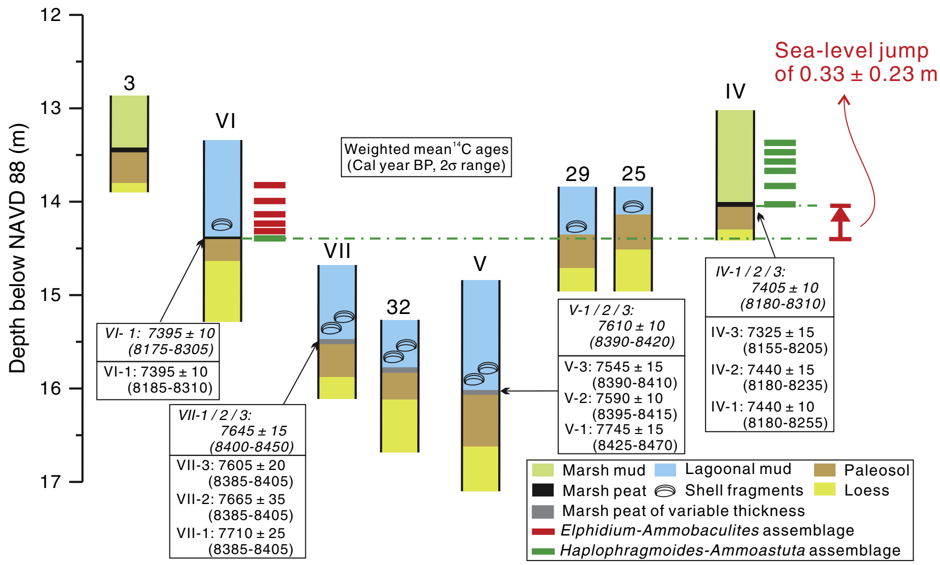

Fig. 2. Stratigraphy and chronology of selected cores from the Bayou Sale area (the complete set of cores is listed in Table 1). Note the striking difference between the deeper portion of the record (sites V, 32, VII, and VI) that features rapid flooding by means of lagoonal mud and the shallower portion (sites IV and 3) that is characterized by persistent marsh facies. Sites VI, 29, 25 and IV capture an abrupt flooding event where the basal-peat beds at sites VI and IV record its onset and end, respectively. Calibration of ^{14}C ages was performed with OxCal (v4.0) for each basal-peat bed, both independently without considering its stratigraphic order (shown in italics in upper box) and by taking into account the stratigraphic order of basal-peat beds (Table 3). NAVD 88 = North American Vertical Datum 88.

The indicative range of basal peat refers to the vertical interval in which basal-peat formation takes place with respect to mean sea level. Van de Plassche (1982) showed that basal-peat accumulation in coastal settings often occurs between mean sea level and mean high water. As shown by the brackish signature of the δ^{13}C and foraminiferal data discussed above, our basal-peat samples formed

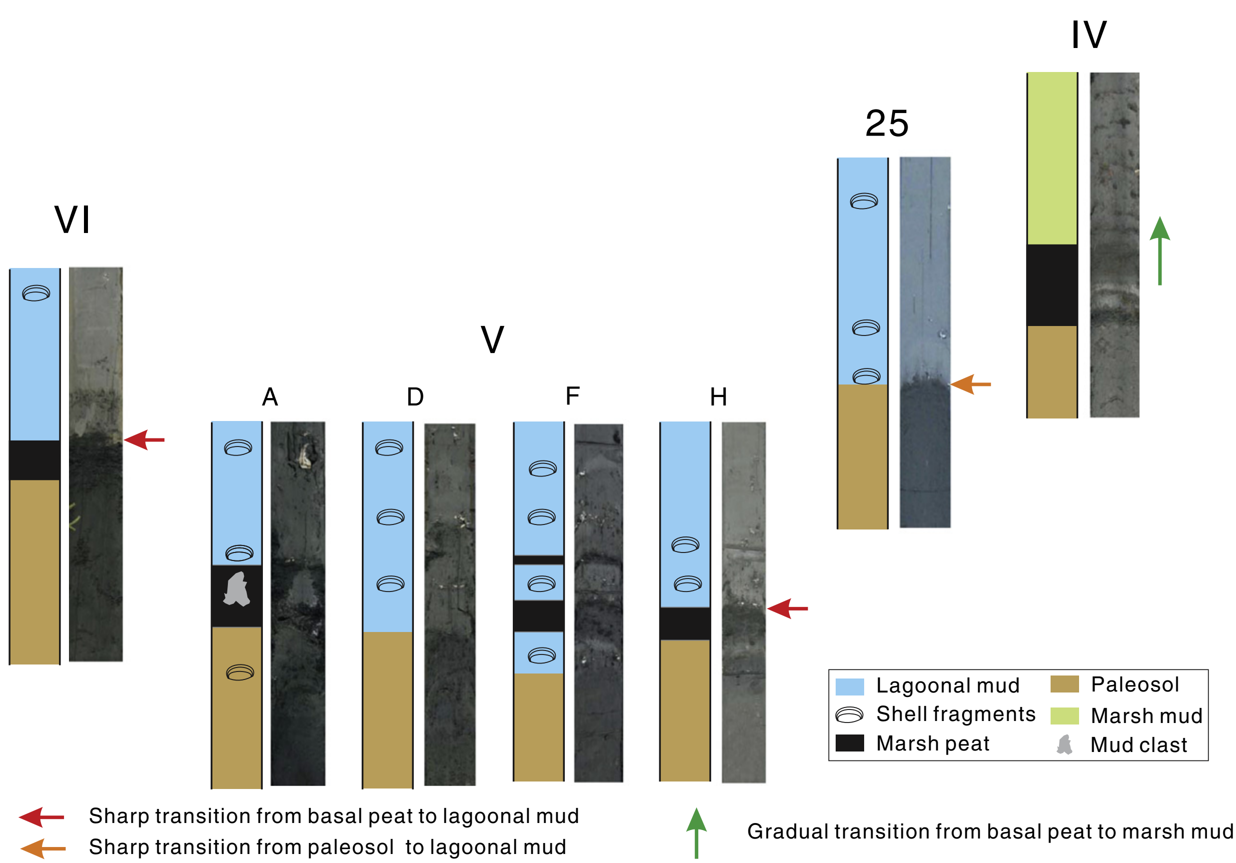

Fig. 3. Photos of representative cores from sites IV, V, VI, and 25. The corresponding stratigraphic column is shown to its left. Photos are arranged to show the relative stratigraphic levels and are not to scale. The diameter of each core is 3.8 cm. Radiocarbon ages of site V were obtained from core H that contains a well preserved basal-peat bed. Note that subtle color differences between cores are partly due to variable light conditions when photos were taken in the field. See text for further details.

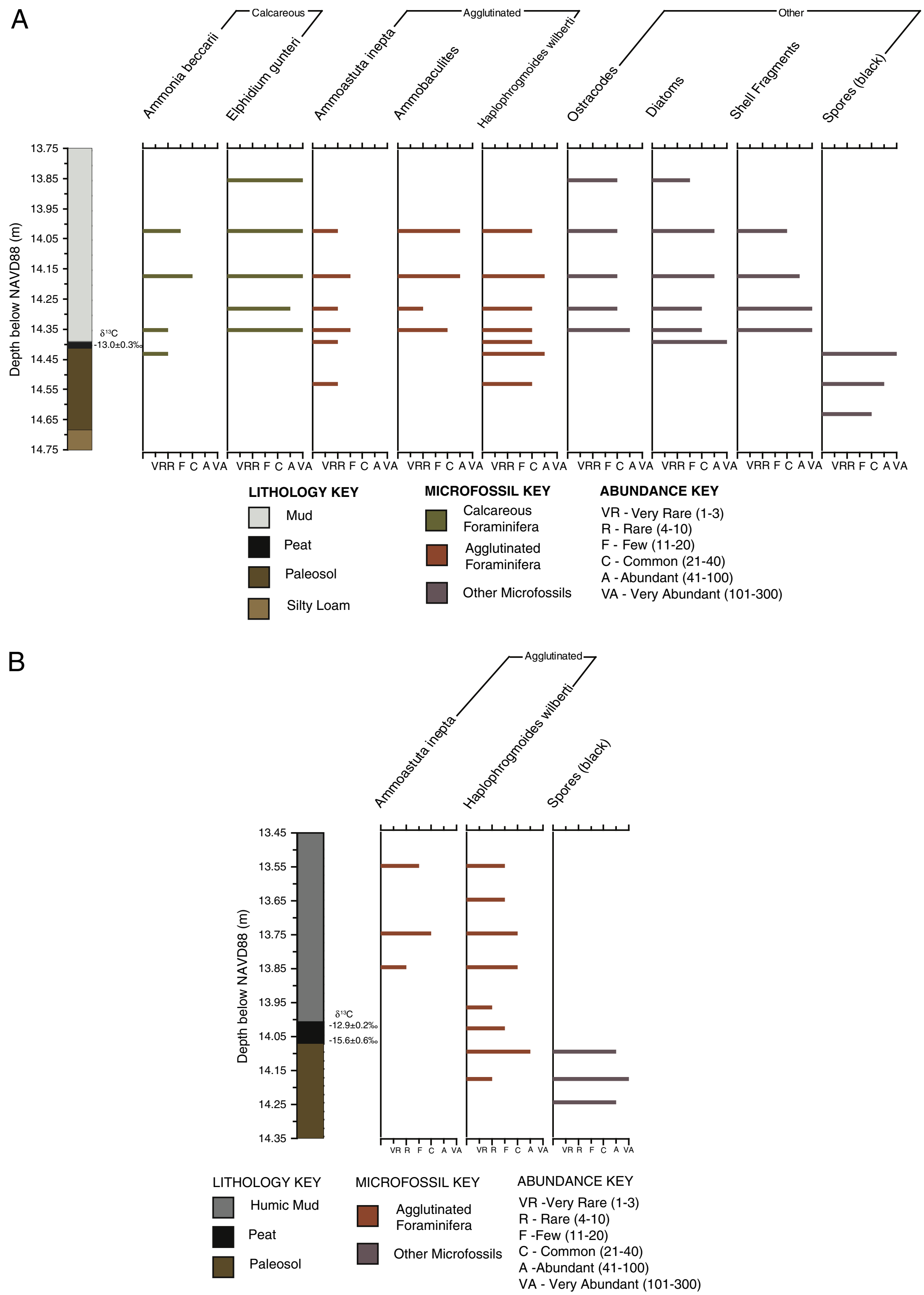

Fig. 4. Summary of the foraminiferal data of representative cores at site VI (A) and site IV (B). See text for further details.

within the intertidal zone. The average present-day spring tidal range in coastal Louisiana is 0.47 m (González and Törnqvist, 2009). Assuming the early Holocene tidal range was comparable to the modern tidal range, the indicative range of the basal peats in our study area would be 0.24 m (cf. González and Törnqvist, 2009). We convert this value to a “two-sided error” of ±0.12 m to be consistent with error designations for depth and elevation measurements.

The cumulative uncertainty of the sea-level elevation inferred from basal peat at each site can be computed with the following equation:

$$E = \sqrt{E_d^2 + E_s^2 + E_{ir}^2}$$

Table 2
Summary of the elevation measurements and uncertainties of the basal peat/paleosol contact at ^{14}C dated sites.

Site	Mean elevation (m)	Number of measurements	E_d (±m)	E_s (±m)	E_{ir} (±m)	E (±m)
Bayou Sale IV	−14.08	10	0.09	0.05	0.12	0.16
Bayou Sale V	−16.07	10	0.10	0.05	0.12	0.16
Bayou Sale VI	−14.41	7	0.10	0.05	0.12	0.16
Bayou Sale VII	−15.53	3	0.05	0.05	0.12	0.14

where E is the total uncertainty; E_d is the depth measurement error; E_s is the surveying error; and E_{ir} is the indicative range error. The elevation measurements and uncertainties are summarized in Table 2.

4.4. Chronology

For each basal-peat bed, different types of terrestrial botanical macrofossils from mostly 2-cm-thick peat intervals were selected for ^{14}C dating. We obtained 21 AMS ^{14}C ages from sites Bayou Sale IV, V, VI, and VII (Table 3). Since cores from sites V and VII show a highly variable stratigraphy within a short distance and some cores (e.g., core D in Fig. 3) even display erosional features, utmost caution was exercised and only well-preserved basal peats were chosen for ^{14}C dating. One ^{14}C measurement (Bayou Sale V-1a) was rejected because it provided a younger age than all stratigraphically higher samples.

The remaining ^{14}C ages were calibrated to calendar years Before Present (BP = AD 1950) using OxCal (v4.0) (Bronk Ramsey, 1995) and

Table 3
Radiocarbon ages of basal peat from the present study in the Bayou Sale area.

Sample name	UTM coordinates[a] (N)	UTM coordinates[a] (E)	Surface elevation (m)	Depth below surface (m)	Material dated	UCIAMS[b] Lab number	Radiocarbon age (^{14}C yr BP ± 1σ)	Radiocarbon age Weighted mean (±1σ)	Calibrated age (cal yr BP) Phase	Weighted mean	2σ range	A index (%)
Bayou Sale IV-1a	3279.02	643.58	0.31	14.37–14.39	11 *Scirpus* spp. achenes	51101	7435 ± 15	7440 ± 10	IV-1	8210	8180–8255	79.8
Bayou Sale IV-1b				14.37–14.39	25 herbaceous charcoal fragments	51102	7440 ± 15					
Bayou Sale IV-2a				14.35–14.37	2 *Scirpus* spp. achenes	51103	7450 ± 60	7440 ± 15	IV-2	8205	8180–8235	60.5
Bayou Sale IV-2b				14.35–14.37	9 herbaceous charcoal fragments	51104	7440 ± 15					
Bayou Sale IV-3a				14.33–14.35	15 *Scirpus* spp. achenes (small)	51105	7315 ± 15	7325 ± 15	IV-3	8180	8155–8205	84.4
Bayou Sale IV-3b				14.33–14.35	7 *Scirpus* spp. achenes (large)	51106	7360 ± 30					
Bayou Sale IV-1/2/3								*7405 ± 10*		*8240*	*8180–8310*	*N/A*
Bayou Sale V-1a	3279.40	644.76	0.33	16.38–16.40	9 *Scirpus* spp. achenes	51107	7270 ± 60[c]	7745 ± 15	V-1	8445	8425–8470	20.4
Bayou Sale V-1b				16.38–16.40	14 herbaceous charcoal fragments	51108	7745 ± 15					
Bayou Sale V-2a				16.36–16.38	17 *Scirpus* spp. achenes	51109	7525 ± 15	7590 ± 10	V-2	8405	8395–8415	59.6
Bayou Sale V-2b				16.36–16.38	14 herbaceous charcoal fragments	51110	7650 ± 15					
Bayou Sale V-3a				16.34–16.36	12 *Scirpus* spp. achenes	51111	7500 ± 15	7545 ± 15	V-3	8400	8390–8410	5.3
Bayou Sale V-3b				16.34–16.36	7 herbaceous charcoal fragments	51112	7670 ± 25					
Bayou Sale V-1/2/3								*7610 ± 10*		*8405*	*8390–8420*	*N/A*
Bayou Sale VI-1a	3281.10	646.08	0.55	14.94–14.96	24 *Scirpus* spp. achenes	51113	7300 ± 15	7395 ± 10	VI-1	8260	8185–8310	78.1
Bayou Sale VI-1b				14.94–14.96	4 large herbaceous charcoal fragments	51114	7430 ± 15					
Bayou Sale VI-1c				14.94–14.96	>30 small herbaceous charcoal fragments	51115	7450 ± 15					
Bayou Sale VI-1								*7395 ± 10*		*8230*	*8175–8305*	*N/A*
Bayou Sale VII-1a	3279.92	644.98	0.41	15.93–15.94	1 large unidentified achene	59674	7710 ± 35	7710 ± 25	VII-1	8395	8385–8405	0.1
Bayou Sale VII-1b				15.93–15.94	2 *Scirpus* spp. achenes, 9 charcoal fragments	59675	7705 ± 35					
Bayou Sale VII-2a				15.91–15.93	10 *Scirpus* spp. achenes (small)	59676	7665 ± 35	7665 ± 35	VII-2	8395	8385–8405	22.1
Bayou Sale VII-2b				15.91–15.93	9 *Scirpus* spp. achenes (large)	59677	7650 ± 120					
Bayou Sale VII-3a				15.89–15.91	11 *Scirpus* spp. achenes (small)	59678	7600 ± 25	7605 ± 20	VII-3	8395	8385–8405	99.7
Bayou Sale VII-3b				15.89–15.91	30 small herbaceous charcoal fragments	59679	7610 ± 25					
Bayou Sale VII-1/2/3								*7645 ± 15*		*8420*	*8400–8450*	*N/A*

[a] UTM coordinates (UTM zone 15R) with reference to North American Datum of 1983 (NAD83).
[b] UCIAMS = University of California, Irvine, accelerator mass spectrometry; Weighted means were obtained with the "combination" function of OxCal (v4.0) (Bronk Ramsey, 1995). Calibrated ages shown in italic were obtained with OxCal by treating each basal peat bed independently without considering their stratigraphic order. For the OxCal sequence analysis approach, the stratigraphic order of basal peat beds is taken into account and a typical 2 cm interval within a basal-peat bed is considered a 'phase' for calibration (VII-1, 1 cm thick).
[c] V-1a is rejected and calibration for V-1 was thus based on V-1b only; Calibrated ages are rounded to the nearest 5 years.

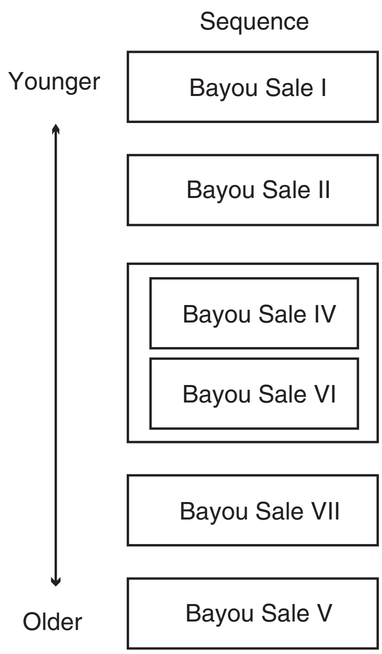

Fig. 5. Model scheme for calibration of radiocarbon ages with the OxCal (v4.0) sequence analysis feature (Bronk Ramsey, 1995). Following the definition for 'sequence' and 'phase' in OxCal, a peat bed is considered a sequence while each 2 cm interval within a peat bed represents a phase. Thus, the bottom, middle, and top 2 cm intervals of a 6-cm-thick peat bed (i.e., a sequence) constitute three phases (e.g., IV-1, IV-2, and IV-3) that are contiguous (i.e., one phase starts immediately after the previous phase has ended, without a time gap). Individual ^{14}C ages from a 2 cm interval (i.e., a phase) are combined to produce a combined age (i.e., a weighted mean) for the corresponding phase using the "^{14}C date combination" option of OxCal. To account for the abrupt flooding event (see Section 5.1), the basal-peat beds at sites VI and IV were grouped together to be considered as one sequence.

the IntCal09 calibration curve (Reimer et al., 2009). Since each basal-peat bed contains multiple ^{14}C ages, we derived calibrated ages using the combination feature of OxCal that calculates weighted mean ^{14}C ages prior to calibration (Table 3). Together with sites I and II from previous studies in the Bayou Sale area (Törnqvist et al., 2004a, 2006), these calibrated ages were used to reconstruct the RSL history for a ~600 yr time span around 8.2 ka (Fig. 6a). In addition, we used the OxCal sequence analysis feature that takes into account the stratigraphic order of basal-peat beds by means of a model scheme (Fig. 5). A quantitative measure of how well the calibrated ages agree with the model scheme is indicated by the "A index". Calibrated ages with an A index over 60% are considered reliable (Bronk Ramsey, 1995). The calibrated ages of peat beds at sites IV through VII are shown in Table 3; the calibrated ages of peat beds at sites I and II are shown in Table 4.

5. Discussion

5.1. Identifying a sea-level jump

While the entire data set (Table 1) exhibits evidence of transgression and RSL rise, only one portion of the record (including sites 25 and 29; Figs. 2, 3) features open-water lagoonal muds that conformably onlap the paleosol with no basal peat. Collectively, sites VI, 25, 29, and IV record an abrupt flooding event that is unlike anything seen elsewhere in our record (Table 1). The sharp transition from basal peat to lagoonal mud at the deeper elevation of site VI marks the onset of this flooding event, while the re-emergence of basal peat at the shallower elevation of site IV registers its end. The absence of basal peat between these two elevations at sites 25 and 29 represents the flooding event itself, when rapidly rising seas prevented coastal marsh from developing and caused direct (conformable) deposition of lagoonal mud over the underlying paleosol. The stratigraphy at sites 25 and 29 is distinctly different from the remainder of the record (Table 1) and suggests a short pulse of near-instantaneous flooding due to extremely rapid sea-level rise. It is unlikely that the distinctive stratigraphy of sites VI, 25, 29, and IV resulted from gradual RSL rise or normal faulting. Had sea level risen gradually, basal peat would occur at sites 25 and 29 as well. Furthermore, recent work (Törnqvist et al., 2006) has shown that fault activity within the study area during the Holocene has been minor.

The OxCal combination approach shows that the basal-peat beds at sites VI and IV yield indistinguishable ages of 8175–8305 and 8180–8310 (2σ) cal yr BP (Fig. 2, Table 3), respectively, indicating that this flooding event occurred within the 8.18–8.31 ka time window. The OxCal sequence analysis approach provides almost similar ages for the basal-peat bed at site VI and the lowermost 2-cm interval (IV-1) of the basal-peat bed at site IV of 8185–8310 and 8180–8255 (2σ) cal yr BP, respectively (Fig. 2, Table 3). This similarity shows that our timing of 8.18–8.31 ka for the sea-level jump is robust.

The mean elevation difference of the basal-peat beds at sites VI and IV is 0.33 m (Table 2) and the associated uncertainty was calculated following

$$\Delta E = \sqrt{E_{VI}^2 + E_{IV}^2}$$

where E_{VI} and E_{IV} are the total uncertainty of the inferred sea level at sites VI and IV, respectively. Since $E_{VI} = E_{IV} = 0.16$ m, $\Delta E = 0.23$ m. Therefore, the magnitude of the sea-level jump recorded between sites VI and IV is 0.33 ± 0.23 m.

5.2. Final Lake Agassiz–Ojibway drainage

The reconstructed early Holocene RSL history (Fig. 6a) suggests slightly higher rates of RSL rise before than after the sea-level jump

Table 4
Radiocarbon ages of basal peat from previous studies (Törnqvist et al., 2004b, 2006) in the Bayou Sale area.

Sample	Surface elevation (m)	Depth below surface (m)	Vertical Error Estimate (m)	Radiocarbon age		Calibrated age (cal yr BP)			
				(^{14}C yr BP ± 1σ)	Weighted mean (± 1σ)	Phase	Weighted mean	2σ range	A index (%)
Bayou Sale I-1[a]	0.27	11.56–11.58	0.33	6997 ± 40		I-1	7865	7755–7940	102.3
Bayou Sale I-1					*6995 ± 40*		*7835*	*7725–7935*	*N/A*
Bayou Sale II-1a[a]	0.48	13.53–13.55	0.35	7480 ± 110	7280 ± 30	II-1	8075	8020–8145	99.9
Bayou Sale II-1b[a]				7265 ± 30					
Bayou Sale II-2[a]		13.50–13.53		7315 ± 60	7315 ± 60	II-2	8070	8010–8140	109.9
Bayou Sale II-1/2					*7290 ± 25*		*8100*	*8025–8170*	*N/A*

Calibrated ages from sites I and II of the previous studies were obtained in the same way as those from sites in this study.
[a] Cores were hand-drilled and the vertical errors also include non-vertical drilling errors of 0.02 m per meter drilled. Weighted mean and calibrated ages are rounded to the nearest 5 years.

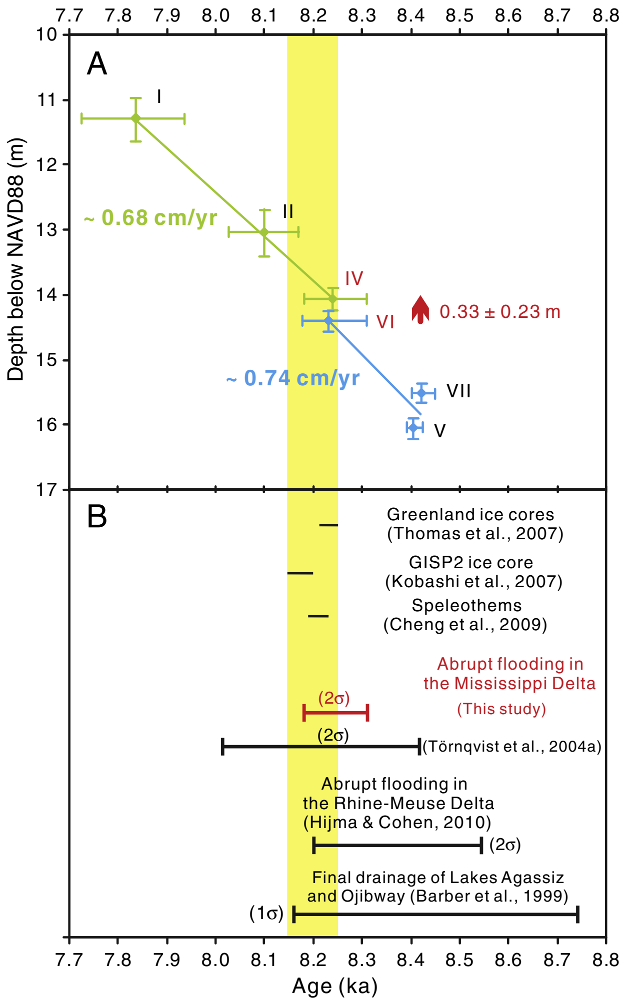

Fig. 6. Relative sea-level (RSL) record and timing of the sea-level jump. (a) The early Holocene RSL record shows a sea-level jump (red arrow) of 0.33 ± 0.23 m between sites VI and IV and RSL rise rates slightly higher before than after the sea-level jump. Note that the identification of this sea-level jump is based on the distinct stratigraphy at sites VI, 25, 29, and IV (Fig. 1). The sea-level index points (SLIPs) in green represent sites where a gradual transition from basal peat to marsh mud occurs. The SLIPs in blue indicate sites where the basal peat was abruptly overlain by brackish-lagoonal mud. Each SLIP is defined by the weighted mean age and the mean elevation of the paleosol/basal peat contact. SLIP ages were obtained with OxCal (v4.0) that calibrated ^{14}C ages for each basal peat bed independently without considering its stratigraphic order. Age error bars indicate the calibrated 2σ age range; calculations of vertical errors are discussed in the text. The green line is a linear regression for sites I, II and IV; the blue line is a linear regression for sites VI, VII, and V. (b) Timing of the onset of the 8.2 ka event (yellow bar) determined from Greenland ice cores and speleothem records from China, Oman, and Brazil, compared to the inferred chronology of 8.18 to 8.31 ka for the final outburst of Lakes Agassiz and Ojibway. The present study reduces the age uncertainty from about 600 years (1σ range) to about 130 years (2σ range). The results of this study refine the previous RSL record (Törnqvist et al., 2004a) around 8.2 ka in the Mississippi Delta.

(~0.74 and ~0.68 cm/yr, respectively). While this difference is subtle and not statistically significant, it is consistent with the markedly different stratigraphic successions prior to and after the sea-level jump. The sharp transition from basal peat to lagoonal mud at sites V, 32, VII, and VI resulted from sudden flooding and marsh drowning. The early portion of our RSL record (sites V, 32, and VII) often exhibits poorly preserved basal peat with large spatial variability over very short distances and abundant evidence of transgressive erosion (Fig. 3, Table 1). We therefore entertain the possibility that episodes of near-instantaneous sea-level rise may have punctuated this phase as well. The sea-level jump recorded at sites VI, 25, 29, and IV represents the final episode of rapid sea-level rise in the early Holocene. The gradual transition from basal peat to marsh mud at sites IV and 3 (Fig. 2) suggests that marsh accretion kept pace with RSL rise after the sea-level jump, which is consistent with the slightly lower rate of RSL rise during this time.

We interpret the sea-level jump within the 8.18–8.31 ka time window as the result of the final LAO outburst. This age range represents the tightest available radiocarbon age constraint on the timing of the final LAO drainage (Fig. 6b). It is important to note that this 130 year time interval arises from the radiocarbon calibration procedure and is thus merely associated with the intrinsic limitations of the dating technique. In addition to the stratigraphic evidence for near-instantaneous drowning, hydraulic modeling has suggested that the flooding associated with the final LAO outburst would have lasted for as little as six months (Clarke et al., 2004). Therefore, this sea-level jump must have occurred as a brief event at any time between 8.18 and 8.31 ka, not as a gradual flooding that persisted for up to 130 years.

The LAO drainage is often believed to have taken place in at least two steps (Dominguez-Villar et al., 2009; Ellison et al., 2006; Leverington et al., 2002). A high-resolution marine record from the North Atlantic reveals two distinct episodes of surface ocean freshening and associated cooling at 8.18–8.34 ka and ~8.49 ka, respectively, suggesting two pulses of freshwater discharge (Ellison et al., 2006). The striking concordance in the timing of the 8.18–8.31 ka sea-level jump and the 8.18–8.34 ka climate anomaly in the North Atlantic suggests that the sea-level jump very likely corresponds to the younger pulse of the LAO drainage (i.e., the final stage of LAO drainage). Since RSL rise prior to the sea-level jump in our study area occurred too rapidly for brackish marsh to be sustained, we cannot rule out the presence of earlier pulses of LAO drainage. For example, the similar ages of basal-peat beds at sites V and VII (Fig. 6a) may indicate such an earlier pulse of freshwater drainage around 8.4 ka, which could potentially correspond to the earlier pulse of ~8.49 ka reported by Ellison et al. (2006) (It should be noted that their age estimate is based on interpolation of limited ^{14}C dating evidence.). We also note that our oldest two samples are consistent with the age of the onset of a sea-level jump (8.54–8.38 ka, 2σ) recently recognized in the Rhine–Meuse Delta (Hijma and Cohen, 2010). Such an earlier freshwater pulse may have pre-conditioned the ocean–atmosphere system (Wiersma and Jongma, 2009), setting the stage for the principal climate event triggered by the final stage of LAO drainage. Our interpretation of a sea-level jump resulting from the final LAO drainage is also consistent with a reconstruction of the properties of the Atlantic inflow that exhibits a pronounced, abrupt freshening of the sub-thermocline at 8.2 ka, interpreted to result from glacial freshwater discharge (Thornalley et al., 2009).

5.3. Volume of the freshwater drainage

The elevation data for sites VI and IV show that the sea-level jump amounted to 0.33 ± 0.23 m (Fig. 2). A maximum of 1.2 ± 0.2 m of abrupt sea-level rise was previously estimated in the study area (Törnqvist et al., 2004a) and was subsequently considered to be dominated by glacial isostatic adjustment (GIA) (Kendall et al., 2008) which is now confirmed by our refined RSL record. These previous studies lacked the stratigraphic details that are currently available (particularly the abrupt flooding evidence from sites 25 and 29) and while GIA was indeed a significant contributor to the overall high rates of early Holocene RSL rise in this region, it was not an appreciable factor for the short-lived sea-level jump identified here.

The sea-level rise of 0.33 ± 0.23 m would mathematically define a range of 0.10 to 0.56 m for the sea-level jump, a value that must be viewed in conjunction with ecological information on marsh resiliency. It is unlikely that 0.1 m of sudden sea-level rise would leave such a widespread stratigraphic signature. Studies of modern coastal ecosystems in the Mississippi Delta (Sasser, 1977) have shown that *Scirpus* spp.-dominated marshes (i.e., comparable to our reconstructed brackish marsh paleoenvironment) occur in the upper portion of the tidal frame and are flooded much less frequently compared to *Spartina alterniflora*-dominated salt marshes (~20 to 160 vs. ~300 times per year, respectively). In other words, given the average present-day spring tidal range for coastal Louisiana of 0.47 m, a substantial sea-level rise is needed to permanently convert a brackish marsh into an open-water lagoon. In addition, coastal marsh plants in microtidal environments like our study area typically have elevation ranges of 0.2 to 0.4 m (Silvestri et al., 2005), and, thus would require a sea-level jump larger than these elevation ranges to enable complete drowning of such ecosystems. In light of these observations, we conservatively adopt a value of 0.2 m as the minimum amount of abrupt sea-level rise. Thus, the sea-level jump around 8.2 ka in our study area amounts to 0.20–0.56 m.

Since the catastrophic LAO drainage would perturb the gravitational field and lead to non-uniform changes in sea level (Kendall et al., 2008), sea-level rise observed in the Mississippi Delta would measure only a fraction of the eustatic sea-level rise (this fraction is known as the fingerprint). The fingerprint value could range from 0.2 if the drainage consisted of LAO freshwater only, to 0.4 if the drainage occurred exclusively as rapidly disintegrating ice over Hudson Bay and Hudson Strait (Kendall et al., 2008). As the contribution from disintegrating ice has been proposed to be relatively small (Clarke et al., 2009), we assume a fingerprint value of 0.25 for the final LAO drainage. The observed sea-level rise of 0.20 to 0.56 m at the Mississippi Delta would then correspond to 0.8 m to 2.2 m of eustatic sea-level rise associated with the final LAO outburst (equivalent to ~3 to 8×10^{14} m^3), exceeding previous estimates for the final LAO drainage (e.g., Barber et al., 1999; Leverington et al., 2002; Törnqvist et al., 2004a). Given the uncertainties in the position of the ice margin of the retreating Laurentide Ice Sheet, the LAO volume may have been larger than the reconstructed 0.45 m sea-level equivalent (SLE) (Leverington et al., 2002) but it is conceivable that the freshwater flux included some Laurentide Ice Sheet melt, likely including icebergs. Therefore, the volume estimate provided here most likely includes both the LAO drainage and discharged icebergs. The relative proportion of these two components, however, is difficult to determine.

A recent study in the Rhine–Meuse Delta inferred a sea-level jump of $\sim 3 \pm 1.25$ m at 8.54–8.2 ka (Hijma and Cohen, 2010). Although the $\sim 3 \pm 1.25$ m SLE is larger than our estimate of 0.8 to 2.2 m SLE, we note that our estimate is exclusively associated with the final stage of LAO drainage, while the $\sim 3 \pm 1.25$ m SLE may well capture multiple pulses of LAO drainage (Hijma and Cohen, 2010). Thus, the two records can potentially be reconciled. Nevertheless, it is the final pulse of LAO drainage that triggered the widespread surface ocean freshening and cooling (Ellison et al., 2006), corresponding to the 8.2 ka climate event as seen in most terrestrial records.

5.4. Implications for abrupt climate change

It has long been postulated that freshwater drainage can trigger abrupt climate events, but large dating uncertainties have prevented causal links from being convincingly established. Our new chronology for the final LAO drainage of 8.18 to 8.31 ka is indistinguishable from the timing of the onset of the 8.2 ka event at 8.15 to 8.25 ka (Cheng et al., 2009; Kobashi et al., 2007; Thomas et al., 2007) (Fig. 6b). This allows for a near-instantaneous ocean–atmosphere response to freshwater forcing, consistent with model predictions (LeGrande et al., 2006; Wiersma and Renssen, 2006). Therefore, our study provides independent chronologic evidence for the hypothesized causal link between the final LAO drainage and the 8.2 ka climate event, and currently constitutes a rare firmly established example of a major abrupt climate change that can be tied directly to a well-identified source of freshwater forcing. The vigorous, ongoing debate regarding such a causal link for other abrupt climate events such as the Younger Dryas (e.g., Broecker et al., 2010; Carlson et al., 2007; Firestone et al., 2007; Lowell et al., 2009) highlights the significance of independent age models for both cause and effect with century-scale or better time resolution.

Finally, the new evidence presented here cannot only inform our understanding of the sensitivity of the MOC to freshwater forcing, but also help improve the accuracy of predictive climate models in the context of future increased ice melt as a result of global warming. Given that the freshwater volume that triggered the 8.2 ka climate event likely amounted to more than 0.8 m of near-instantaneous eustatic sea-level rise, our findings lend support to the notion (Meehl et al., 2007) that abrupt cooling due to global warming in the next century is relatively unlikely.

6. Conclusions

We present a high-resolution early Holocene sea-level record from the Mississippi Delta that documents a distinct sea-level jump, marked by a characteristic stratigraphic succession that is corroborated by paleoenvironmental reconstruction. The 0.20–0.56 m local sea-level jump occurred within the 8.18 to 8.31 ka (2σ) time window and is attributed to the final drainage of proglacial Lake Agassiz–Ojibway (LAO). Since the timing of the sea-level jump is indistinguishable from the onset of the 8.2 ka climate event, this study provides compelling evidence for a nearly immediate ocean–atmosphere response to the freshwater perturbation.

In addition, the total inferred eustatic sea-level rise at 8.2 ka (after correction for gravitational effects) amounts to 0.8 to 2.2 m, considerably higher than previous estimates for the final stage of LAO drainage. The new constraints on the timing and amount of final LAO drainage provide additional insight into the sensitivity of MOC to freshwater perturbation, a crucial step toward understanding abrupt climate change. For example, our findings support the notion that abrupt cooling due to global warming in the next century is relatively unlikely.

Acknowledgements

Mike Blum (Louisiana State University) kindly made his Geoprobe drilling system available for this study. Zhixiong Shen, Shiyong Yu, Juan González, and Floyd DeMers are thanked for field assistance and land owners Debi Lauret and Antoine Luke for providing access to their property. We are grateful to John Southon and his staff for radiocarbon dating, to Brad Rosenheim for help with the stable carbon isotope analysis, and to Hans Renssen, Marc Hijma, Sergio Fagherazzi, Irv Mendelssohn, and George Flowers for elucidating discussion. Comments by two referees significantly improved the manuscript. Funding for this study was provided by the Earth System History program of the U.S. National Science Foundation (OCE-0601814) and the McWilliams Fund of the Department of Earth and Environmental Sciences, Tulane University.

References

Alley, R.B., Ágústsdóttir, A.M., 2005. The 8 k event: cause and consequences of a major Holocene abrupt climate change. Quat. Sci. Rev. 24, 1123–1149.
Alley, R.B., et al., 2003. Abrupt climate change. Science 299, 2005–2010. doi:10.1126/science.1081056.
Autin, W.J., et al., 1991. Quaternary geology of the Lower Mississippi Valley. In: Morrison, R.B. (Ed.), Quaternary Nonglacial Geology: Conterminous U.S.: Geological Society of America: The Geology of North America, K-2, pp. 547–582.
Barber, D.C., et al., 1999. Forcing of the cold event 8200 yr ago by catastrophic drainage of laurentide lakes. Nature 400, 344–348.
Broecker, W.S., et al., 1989. Routing of meltwater from Laurentide Ice Sheet during the Younger Dryas cold episode. Nature 314, 318–321.
Broecker, W.S., et al., 2010. Putting the Younger Dryas cold event into context. Quat. Sci. Rev. 29, 1078–1081. doi:10.1016/j.quascirev.2010.02.019.

Bronk Ramsey, C., 1995. Radiocarbon calibration and analysis of stratigraphy: the OxCal program. Radiocarbon 37, 425–430.
Carlson, A.E., et al., 2007. Geochemical proxies of North American freshwater routing during the Younger Dryas cold event. Proc. Natl. Acad. Sci. 104, 6556–6561.
Carlson, A.E., Clark, P.U., Haley, B.A., Klinkhammer, G.P., 2009. Routing of western Canadian Plains runoff during the 8.2 ka cold event. Geophys. Res. Lett. 36, L14704. doi:10.1029/2009GL038778, 2009.
Cheng, H., et al., 2009. Timing and structure of the 8.2 kyr event inferred from ^{18}O records of stalagmites from China, Oman, and Brazil. Geology 37, 1007–1010.
Chmura, G.L., Aharon, P., Socki, R.A., Abernethy, R., 1987. An inventory of ^{13}C abundances in coastal wetlands of Louisiana, USA: vegetation and sediments. Oecologia 74, 264–271.
Clarke, G.K.C., Leverington, D.W., Teller, J.T., Dyke, A.S., 2004. Paleohydraulics of the last outburst flood from glacial Lake Agassiz and the 8200 BP cold event. Quat. Sci. Rev. 23, 389–407.
Clarke, G.K., Bush, A.B.G., Bush, J.W.M., 2009. Freshwater discharge, sediment transport, and modeled climate impacts of the final drainage of glacial lake Agassiz. J. Clim. 22, 2161–2180.
Clement, A.C., Peterson, L.C., 2008. Mechanisms of abrupt climate change in the last glacial period. Rev. Geophys. 46, RG4002 Paper number 2006RG000204.
Dominguez-Villar, D., et al., 2009. Oxygen isotope precipitation anomaly in the North Atlantic region during the 8.2 ka event. Geology 37, 1095–1098.
Donnelly, J.P., Cleary, P., Newby, P., Ettinger, R., 2004. Coupling instrumental and geological records of sea-level change: evidence from southern New England of an increase in the rate of sea-level rise in the late 19th century. Geophys. Res. Lett. 31, L05203. doi:10.1029/2003GL018933.
Ellison, C.R.W., Chapman, M.R., Hall, I.R., 2006. Surface and deep ocean interactions during the cold climate event 8200 years ago. Science 312, 1929–1932.
Firestone, R.B., et al., 2007. Evidence for an extraterrestrial impact 12,900 years ago that contributed to the megafaunal extinctions and the Younger Dryas cooling. Proc. Natl. Acad. Sci. 104, 1616–1621.
Fisher, T.G., Yansa, C.H., Lowell, T.V., Lepper, K., Hajdas, I., Ashworth, A.C., 2008. The chronology, climate, and confusion of the Moorhead Phase of Glacial Lake Agassiz: new results from the Ojata Beach, North Dakota, U.S.A. Quat. Sci. Rev. 27, 1124–1135.
González, J.L., Törnqvist, T.E., 2009. A new Holocene sea-level record from the Mississippi Delta: evidence for a climate/sea level connection? Quat. Sci. Rev. 28, 1737–1749.
Heinrich, H., 1988. Origin and consequences of cyclic ice rafting in the northeast Atlantic Ocean during the past 130,000 years. Quat. Res. 29, 142–152.
Hijma, M.P., Cohen, K.M., 2010. Timing and magnitude of the sea-level jump preluding the 8200 yr event. Geology 38, 275–278.
Jelgersma, S., 1961. Holocene sea level changes in the Netherlands. Meded. Geol. Sticht. Ser. C 6 (7), 1–100.
Kane, H.E., 1967. Recent microfaunal biofacies in Sabine Lake and environs, Texas and Louisiana. J. Paleontol. 41, 947–964.
Kendall, R.A., Mitrovica, J.X., Milne, G.A., Törnqvist, T.E., Li, Y.X., 2008. The sea-level fingerprint of the 8.2 ka climate event. Geology 36, 423–426.
Kleiven, H.F., et al., 2008. Reduced North Atlantic deep water coeval with the glacial Lake Agassiz freshwater outburst. Science 319, 60–64.
Kobashi, T., Severinghaus, J.P., Brook, E.J., Barnola, J.-M., Grachev, A.M., 2007. Precise timing and characterization of abrupt climate change 8200 years ago from air trapped in polar ice. Quat. Sci. Rev. 26, 1212–1222.
Lajeunesse, P., St-Onge, G., 2008. The subglacial origin of the Lake Agassiz–Ojibway final outburst flood. Nat. Geosci. 1, 184–188. doi:10.1038/ngeo130.
LaSalle, M.W., de la Cruz, A.A., 1985. Species profiles: life histories and environmental requirements of coastal fishes and invertebrates (Gulf of Mexico): common rangia. US Fish Wildl. Serv. Biol. Rep. 82 (11.31) US Army Corps of Engineers, TR EL-82-4: 16 pp.
LeGrande, A.N., et al., 2006. Consistent simulations of multiple proxy responses to an abrupt climate change event. Proc. Natl. Acad. Sci. 103, 837–842.
Leverington, D.W., Mann, J.D., Teller, J.T., 2002. Changes in the bathymetry and volume of glacial Lake Agassiz between 9200 and 7700 ^{14}C yr B.P. Quat. Res. 57, 244–252.
Lowell, T.V., et al., 2009. Radiocarbon deglaciation chronology of the Thunder Bay, Ontario area and implications for ice sheet retreat patterns. Quat. Sci. Rev. 28, 1597–1607.
Meehl, G.A., et al., 2007. Global Climate Projections. In: Solomon, S., Qin, D., Manning, M., Chen, Z., Marquis, M., Averyt, K.B., Tignor, M., Miller, H.L. (Eds.), Climate Change 2007: The Physical Science Basis. Contribution of Working Group I to the Fourth Assessment Report of the Intergovernmental Panel on Climate Change. Cambridge University Press, Cambridge, United Kingdom and New York, NY, USA.
Muscheler, R., Beer, J., Vonmoos, M., 2004. Causes and timing of the 8200 yr BP event inferred from the comparison of the GRIP ^{10}Be and the tree ring $\Delta^{14}C$ record. Quat. Sci. Rev. 23, 2101–2111.
Parker, R.H., 1959. Macro-invertebrate assemblages of central Texas coastal bays and Laguna Madre. Am. Assoc. Pet. Geol. Bull. 43, 2100–2166.
Phleger, F.B., 1965. Patterns of Marsh Foraminifera, Galveston Bay, Texas. Limnol. Oceanogr. 10, R169–R184 (Suppl.).
Reimer, P.J., Baillie, M.G.L., Bard, E., et al., 2009. IntCal09 and Marine09 radiocarbon age calibration curves, 0–50,000 years cal BP. Radiocarbon 51, 1111–1150.
Rohling, E.J., Pälike, H., 2005. Centennial-scale climate cooling with a sudden cold event around 8,200 years ago. Nature 434, 975–979.
Sasser, C.E. 1977. Distribution of vegetation in Louisiana coastal marshes as response to tidal flooding. M.S. thesis, Louisiana State University.
Scott, D.B., Suter, J.R., Kosters, E.C., 1991. Marsh Foraminifera and arcellaceans of the lower Mississippi Delta: Controls on spatial distributions. Micropaleontology 37, 373–392.
Silvestri, S., Defina, A., Marani, M., 2005. Tidal regime, salinity and salt marsh plant zonation. Estuarine Coastal Shelf Sci. 62, 119–130.
Thomas, E.R., et al., 2007. The 8.2 ka event from Greenland ice cores. Quat. Sci. Rev. 26, 70–81.
Thornalley, R.J.R., Elderfield, H., McCave, I.N., 2009. Holocene oscillations in temperature and salinity of the surface subpolar North Atlantic. Nature 457, 711–714.
Törnqvist, T.E., Bick, S.J., González, J.L., Van der Borg, K., De Jong, A.F.M., 2004a. Tracking the sea-level signature of the 8.2 ka cooling event: new constraints from the Mississippi Delta. Geophys. Res. Lett. 31, L23309. doi:10.1029/2004GL021429.
Törnqvist, T.E., et al., 2004b. Deciphering Holocene sea-level history on the U.S. Gulf Coast: a high resolution record from the Mississippi Delta. Geol. Soc. Am. Bull. 116, 1026–1039. doi:10.1130/B2525 478.1.
Törnqvist, T.E., Bick, S.J., Van der Borg, K., De Jong, A.F.M., 2006. How stable is the Mississippi Delta? Geology 34, 697–700.
Van de Plassche, O., 1982. Sea-level change and water-level movements in the Netherlands during the Holocene. Meded. Rijks Geol. Dienst. 36, 1–93.
Van de Plassche, O., 1986. Introduction. In: Van de Plassche, O. (Ed.), Sea-Level Research: a Manual for the Collection and Evaluation of Data. Geo Books, Norwich, pp. 1–26.
Wiersma, A.P., Jongma, J.I., 2009. A role for icebergs in the 8.2 ka climate event. Clim. Dyn. 35, 535–549. doi:10.1007/s00382-009-0645-1.
Wiersma, A.P., Renssen, H., 2006. Model-data comparison for the 8.2 ka BP event: confirmation of a forcing mechanism by catastrophic drainage of Laurentide Lakes. Quat. Sci. Rev. 25, 63–88.